

# Deposition of charged nano-particles in the human airways including effects from cartilaginous rings

Hans O. Åkerstedt

Department of Applied Physics and Mechanical Engineering, Luleå University of Technology, Luleå, Sweden;  
[hake@ltu.se](mailto:hake@ltu.se)

Received 17 August 2011; revised 20 September 2011; accepted 28 September 2011.

## ABSTRACT

This paper presents a numerical study of the deposition of spherical charged nano-particles caused by convection, Brownian diffusion and electrostatics in a pipe with a cartilaginous ring structure. The model describes the deposition of charged particles in the different generations of the tracheobronchial tree of the human lung. The upper airways are characterized by a certain wall structure called cartilaginous rings which modify the particle deposition when compared to an airway with a smooth wall. The problem is defined by solving Navier-Stokes equations in combination with a convective-diffusion equation and Gauss law for electrostatics. Three non-dimensional parameters describe the problem, the Peclet number  $Pe = 2\bar{U}a/D$ , the Reynolds number  $Re = 2\bar{U}a/\nu$  and an electrostatic parameter  $\alpha = a^2 c_0 q^2 / (4\epsilon_0 \kappa T)$ . Here  $U$  is the mean velocity,  $a$  the pipe radius and  $D$  the diffusion coefficient due to Brownian motion given by  $D = \kappa T Cu / 3\pi\mu d$ , where  $Cu$  is the Cunningham-factor  $Cu = 1 + \lambda/d (2.34 + 1.05 \exp(-0.39d/\lambda))$ . Here  $d$  is the particle diameter and  $\lambda$  the mean free path of the air molecules. Results are provided for generations G4-G16 of the human airways. The electrostatic parameter is varied to model different concentrations and charge numbers.

**Keywords:** Charged Particles; Nanoparticles; Convection; Brownian Motion; Deposition; Respiratory Airways; Cartilaginous Rings

## 1. INTRODUCTION

Use of Carbon-nanotubes in material design enables the development of new materials with superior properties. A drawback of this development is that these particles when inhaled may be toxic and can cause substan-

tial health risks of the human lung [1]. In experiments these particles are known to be electrically charged which probably leads to an increase in particle deposition in the lung. Another important application of charged nano-particles is in the design of methods for optimal drug-aerosol targeting to predetermined lung sites [2].

The morphology of the human respiratory airways of the human lung is represented by a system of branching tubes where each tube belongs to a certain generation [3]. The first tube labeled generation zero (G0) is a single tube called trachea. After the trachea the tube bifurcates into two tubes of generation 1 (G1). Beyond generation G16 we have the alveolar region (generation G17-G23), which consists of tubes with multiple sacs (the alveoli) expanding and contracting periodically during the breathing cycle. This is the region where the gas exchange takes place with the blood-vessel system.

In the present paper we analyze how nano-particles are deposited in the human lung airways and especially we consider the effects caused by charged nanoparticles. We also include the wall structure of the upper airways called cartilaginous rings.

For low space-charge densities the dominant transport mechanism is the electric field that occurs from the image charge caused by the interaction of a particle and a grounded wall. This case has been studied by [4-6].

For a large number of particles, however, the transport to the wall is dominated by the mutual electrical repulsion of the charged particles. This case has been analyzed by [5,7].

To find the transport and particle deposition in general flow geometry there are essentially two methods. One method is to solve the equations of motion of the particles in the flow field which is generated by solutions of Navier-Stokes equation [8]. To get statistical measures of the deposition a large number of particles ( $N$ ) need to be simulated with an error of the order  $O(N^{-1/2})$ . This approach is difficult if we wish to find the electric field and transport from a high concentration of particles. An alternative method is to more directly consider the equa-

tion that describe the probability density of the particles, *i.e.* the Fokker-Planck equation (Risken (1976) [9], Åkerstedt *et al.* (2010) [10]) or a convective diffusion equation for the concentration (Åkerstedt *et al.* (2010) [11]).

In the present paper we consider this latter approach of solving the convective-diffusion equation combined with Navier-Stokes equations for the fluid flow and Poisson's equation for the electrostatic field. We consider the situation where the space-charge density is large so that the transport mechanism is dominated by the electric field due to charge repulsion. In previous studies [5,7,12] of this case fully developed fluid flow is assumed. This is a good approximation for the higher generations (>G10) of the airways, but for the upper lower generation airways, the effect of a developing fluid flow is important. In this paper where we consider generations G4 - G16 we therefore assume the fluid to develop from a uniform velocity profile at entry. We also consider the additional effects of the cartilaginous ring wall structure.

## 2. GOVERNING EQUATIONS

Each generation of the human airways is supposed to be described by a tube with a smooth surface or with a cartilaginous ring structure (**Figure 1**). For the individual airways of each generation we assume axial symmetry. The following set of equations describes the physics of the problem.

$$(\mathbf{u} \cdot \nabla) \mathbf{u} = -\nabla p + \frac{1}{Re} \nabla^2 \mathbf{u} \tag{1a}$$

$$\nabla \cdot \mathbf{u} = 0 \tag{1b}$$

$$(\mathbf{u} \cdot \nabla) c - \frac{1}{Pe} \nabla \phi \cdot \nabla c + 4\alpha \frac{c^2}{Pe} = \frac{1}{Pe} \nabla^2 c \tag{1c}$$

$$\nabla^2 \phi = -4\alpha c \tag{1d}$$

The dimensionless parameters of the problem are the Reynolds number, the Peclet-number and an electrostatic parameter.

$$\begin{aligned} Re &= \frac{\bar{U} 2a}{\nu} \\ Pe &= \frac{\bar{U} 2a}{D} \\ \alpha &= \frac{1}{4} \frac{c_0 q^2 a^2}{\epsilon_0 \kappa T} \end{aligned} \tag{2}$$

Here  $\bar{U}$  is the mean uniform velocity at inlet and  $a$  is the pipe radius,  $\nu$  is the kinematic viscosity of air and  $D$  is the Brownian diffusion constant defined as

$$\begin{aligned} D &= \frac{\kappa T Cu}{3\pi\mu d} \\ Cu &= 1 + \frac{\lambda}{d} \left( 2.34 + 1.05 \exp\left(-0.39 \frac{d}{\lambda}\right) \right) \end{aligned} \tag{3}$$

where  $Cu$  is the Cunningham factor which is a correction factor needed to bridge the gap between the continuum limit and the free molecular limit for the flow past a sphere. Here  $\lambda$  is the collision mean free path and  $d$  is the particle diameter.  $\kappa$  is Boltzmanns constant,  $T$  is the absolute temperature and  $\mu$  is the dynamic viscosity of the air. The charge of the particles is  $q$  and the concentration of particles at inlet is  $c_0$ .

**Eq.1c** is an equation describing the evolution of the concentration  $c$ , which is an equation of convective-diffusion type with an extra source-term including the effects from the electric field. **Eqs.1a** and **1b** are the Navier-Stokes equations describing the evolution of the laminar fluid flow and **Eq.1d** is Poisson's equation which gives the link between the charged particles and the electric field.

The set of **Eqs.1a-1d** needs to be solved together numerically as a system and for this purpose we use the commercial software Comsol Multiphysics 4.2. The application modes in Comsol that have been applied are stationary Navier-Stokes, stationary transport of diluted species (convective-diffusion equation) and electrostatics. The boundary conditions for the fluid flow are no slip on the pipe wall  $r = a$ . At the inlet  $x = 0$  a uniform velocity is chosen and at  $x = L$  outlet conditions are applied. For the application of the diffusion-convection mode, the concentration at the inlet is uniform  $c = c_0$ .

The boundary condition of the absorbing wall is  $c = 0$  and at the outlet convective flux is chosen. For the electrostatics mode, zero charge/symmetry is chosen at the inlet and outlet. Since the wall at  $r = a$  of the respiratory airways consists of a so called mucus-layer including mainly saline water, the wall is treated as a good conductor and therefore the electric potential is taken as zero. For the meshing we apply the extremely fine physics-controlled mesh supplied by the software.

## 3. NUMERICAL RESULTS

We have chosen to provide numerical results from generation G4-G16 for which the airway has a ring structure with an amplitude of 0.1 diameters [13,14] (**Figure 1**). In generations G4 - G16 the flow is usually laminar in contrast with the upper generations G0 - G3 which is usually characterized by turbulent flow.

The deposition of particles is calculated using the total flux of particles out of the tube  $\Gamma_2$  and the total flux of particles into the tube  $\Gamma_1$  which are defined as

$$\Gamma_j = \int_{S_j} c \mathbf{u} \cdot \hat{n} dS - \frac{1}{Pe} \int_{S_j} \nabla c \cdot \hat{n} dS - \frac{1}{Pe} \int_{S_j} \nabla \phi \cdot \hat{n} dS \tag{4}$$

Here  $\hat{n}$  is the unit normal out of the tube surfaces  $S_j, j = 1, 2$ . The first terms in (4) correspond to convec-

tive flux, the second to Brownian diffusion flux and the third to electrical mobility flux. Since the  $Pe$ -number is usually large the convective flux dominates.

The deposition is then calculated from

$$P = 1 + \frac{\Gamma_2}{\Gamma_1} \quad (5)$$

We first discuss some results for the tube of airway generation G4 with uncharged particles. For light breathing conditions we have a mean velocity of 1.47 m/s. The tube radius is 2.25 mm and the length of the pipe is 12.4 mm. The Reynolds number is then  $Re = 348$ . We chose a particle with a diameter of 10 nm, which gives a Peclet-number of  $Pe = 1.41 \cdot 10^5$ .

In **Figures 1** and **2** the result for generation G4 is presented. The distribution of concentration and the streamlines are shown. In the figures fluid enters from the top with uniform velocity and uniform concentration  $c_0$ . In the figures high concentration corresponds to red color and low concentration to blue color. From the behavior of the streamlines it is noted that the flow separates in the regions between the rings. In the separated regions the concentration is about half the concentration at inlet.

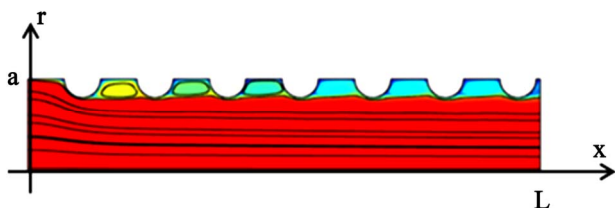


**Figure 1.** Tube with a cartilaginous ring wall structure. Concentration and streamlines. Red color denotes high concentration and blue color low concentration. Fluid and particles enter from the left at  $x = 0$ .

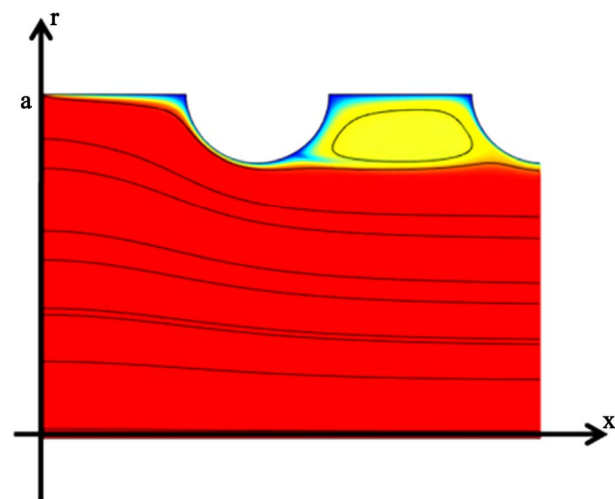


**Figure 2.** Concentration and streamlines close to entry of G4. Red color denotes high concentration and blue color low concentration. Fluid and particles enter from the left  $x = 0$ .

In general the local Brownian diffusion flux or particle deposition is smaller in the separated regions with a maximum deposition at the point of reattachment of the fluid flow. More details of this case for uncharged particles have been presented by Åkerstedt *et al.* (2010) [11].

Next we consider the effect of charged particles. For a large number of particles the transport to the wall is dominated by the mutual electrical repulsion effect. The dimensionless parameter that describes this space-charge electrostatic effect is

$$\alpha = \frac{1}{4} \frac{c_0 q^2 a^2}{\epsilon_0 \kappa T}$$

Here  $c_0$  is the concentration of particles at the inlet and  $q$  is the charge of the particles.

As an example for generation G4 with a tube radius of 2.25 mm and particles that carry 10 elementary charges and where the particle concentration at inlet is  $10^{11}$  particles/m<sup>3</sup> the electrostatic parameter is  $\alpha = 8.5$ .

In **Figure 3** the upper part of the tube of generation G4 is shown for  $\alpha = 100$ . Here the arrows correspond to the electric field and the color to the norm of the electric field. It is noted that the electric field is weaker in the regions between the rings, *i.e.* in the regions of separated flow. This can be explained by the lower values of concentration in the separated regions (see **Figure 2**).

This also has some consequences also for the amount of particles deposited to the wall. In **Figure 4** the particle deposition is plotted for generation G4 for different values of the parameter  $\alpha$ . For comparison the deposition for a smooth tube is also presented.

We note that the deposition is lower for a tube with a cartilaginous ring structure, which can be explained by the lower concentration of particles and the lower values of the electric field in the separated flow regions.

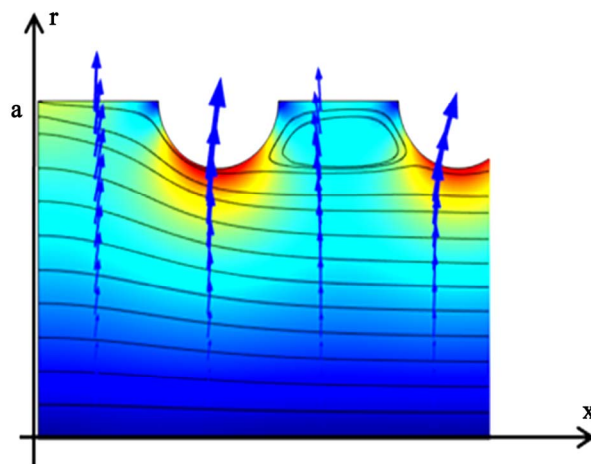


**Figure 3.** Red color indicates high electric field and blue low electric field. Arrows of the electric field and the streamlines close to entry of G4.

The amount of deposition can be controlled to a great extent with the value of the parameter  $\alpha$ , which in turn depends on the concentration at entry  $c_0$  and the square of the charge of the particles  $q$ .

This result may be of importance in the application of designing charged nano-particles for optimal drug-aerosol targeting to predetermined lung sites. For generation G4 although the deposition rates are small, we note that increasing the parameter  $\alpha$  from zero to 350 the deposition increases by 80%. It is expected that this effect is larger for higher generations. Therefore it is of interest to consider particle deposition also for generations G6 to G16.

In **Figure 5** the particle deposition as a function of the parameter  $\alpha$  is presented for generations G6 - G10 and in **Figure 6** the corresponding deposition is presented for generations G12 - G16.

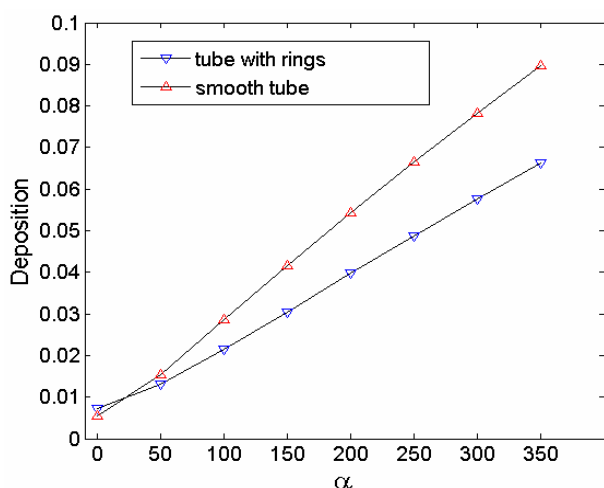


**Figure 4.** Deposition for different values of  $\alpha$  for a smooth walled tube and a tube with cartilaginous rings. Generation G4.

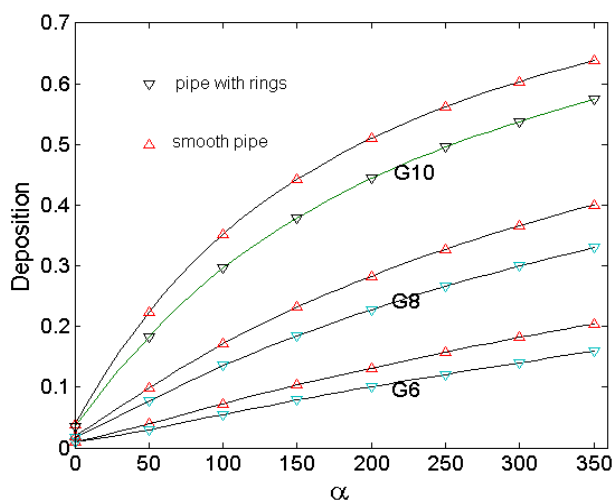


**Figure 5.** Deposition for different values of  $\alpha$  for a smooth walled tube and a tube with cartilaginous rings. Generations G12 - 16.

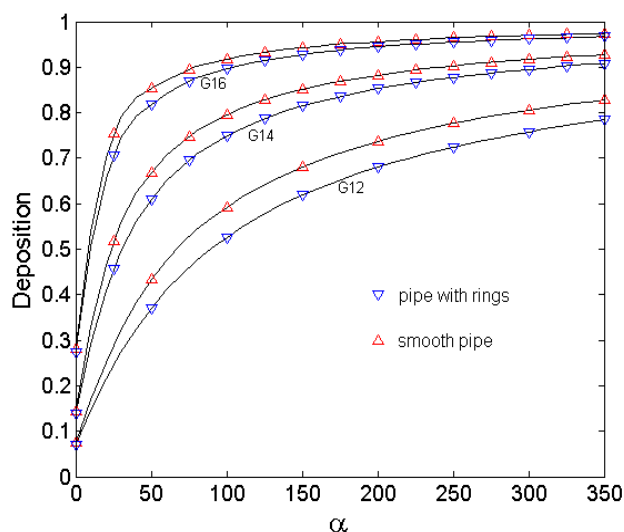


**Figure 6.** Deposition for different values of  $\alpha$  for a smooth walled tube and a tube with cartilaginous rings. Generations G12 - 16.

We note that there is a considerable increase in the deposition for large values of  $\alpha$  especially for the higher generations for which even a rather small value of  $\alpha$  leads to considerable deposition. We also note that the presence of the cartilaginous rings only leads to a slight decrease in the deposition. The effect of these rings is probably larger for particles of micron size and for lower generations which has been observed in model experiments of the upper airways [13].

#### 4. CONCLUSIONS AND DISCUSSION

The deposition of nano-sized charged spherical particles on the walls of cylindrical tube with a periodically spaced cartilaginous ring structure is investigated. The model includes convective and Brownian diffusion transport as well as effects from the electric field created by the charged particles.

The deposition of charged particles depends to a large extent upon the single parameter  $\alpha$ , which includes the concentration at inlet, the particle charge and the particle radius. For the higher generations G14 - 16 and large  $\alpha$  the deposition is as large as 80% - 90%, so almost all particles are deposited. The effect of the cartilaginous is in general to decrease the deposition, which can be explained by the separation of the flow in the regions between the rings. In the separated area the concentration is about half the concentration at inlet which gives a smaller electric field in these areas and therefore also leads to less deposition. The reduction of deposition due to the cartilaginous rings is in general not large with the largest reduction of about 30% for G4 and almost no reduction for G16.

Due to decisive role of the parameter  $\alpha$  for deposition, these results should be useful for manufactures of inhaler-devices in their strive for optimal design of therapeutic aerosols.

To validate the results experimentally is extremely difficult especially in vivo measurements of nano-particles in the higher generations. As mentioned earlier a physical model of the first two generations including a cartilaginous wall structure has been conducted for micron particles [13]. The behavior of micron particles is however quite different than for nano-particles. The latter are also much more difficult to detect. So up to the knowledge of the author there are no known results which can be used for validation of the present numerical results.

Future work involves studying the lower generations G0 - G3 where the flow may become turbulent. This analysis requires the use of a low-Reynolds-number turbulence model for the flow and a modification of the convective-diffusion equation to include turbulent diffusion. Of interest is also the study of larger particles of micron-size, for which the alternative technique of Lagrangian tracking is a more suitable approach. (Högberg *et al.* [8]).

For validation of deposition of nano-particles in simple geometries, we will also consider a recent technique to track the individual transport of particles using digital holography [14].

## 5. ACKNOWLEDGEMENTS

This work is sponsored by the Swedish research council, Swedish Agency for Economic and Regional Growth and Centre for biomedical engineering and physics.

## REFERENCES

- [1] Poland, C.A., Duffin, R., Kinloch, I. Maynard, A., Wallace, W.A.H., Seaton, A., Stone, V., Brown, S., Macnee, W. and Donaldson, K. (2008) Carbon nanotubes introduced into the abdominal cavity of mice show asbestos-like pathogenicity in a pilot study. *Nature nanotechnology*, **3**, 423-428. [doi:10.1038/nnano.2008.111](https://doi.org/10.1038/nnano.2008.111)
- [2] Kleinstreuer, C., Zhang, Z., Donohue, J.F. (2008) Targeted drug-aerosol delivery in the human respiratory system. *Annual Review of Biomedical Engineering*, **10**, 195-220. [doi:10.1146/annurev.bioeng.10.061807.160544](https://doi.org/10.1146/annurev.bioeng.10.061807.160544)
- [3] Weibel, E. R. (1963). Morphometry of the human lung. Academic Press, New York.
- [4] Yu, C.P. (1977) Precipitation of unipolarly charged particles in cylindrical and spherical vessels. *Journal of Aerosol Science*, **8**, 237-241. [doi:10.1016/0021-8502\(77\)90043-X](https://doi.org/10.1016/0021-8502(77)90043-X)
- [5] Yu, C.P. and Chandra, K. (1977) Precipitation of submicron charged particles in human lung airways. *Bulletin of Mathematical Biology*, **39**, 471-478.
- [6] Becker, R.S., Anderson, V.E., Allen, J.D., Birkhoff, R.D. and Ferrell, T.L. (1980) Electrical image deposition of charges from laminar flow in cylinders. *Journal of Aerosol Science*, **11**, 461-466. [doi:10.1016/0021-8502\(80\)90118-4](https://doi.org/10.1016/0021-8502(80)90118-4)
- [7] Ingham, D.B. (1980) Deposition of charged particles near the entrance of a cylindrical tube. *Journal of Aerosol Science*, **12**, 47-52. [doi:10.1016/0021-8502\(80\)90143-3](https://doi.org/10.1016/0021-8502(80)90143-3)
- [8] Högberg, S.M., Åkerstedt, H.O., Lundström, T.S. and Freund J. (2010) Respiratory deposition of fibers in the non-inertial regime: Development and application of a semi-analytical model. *Aerosol Science and Technology*, **44**, 847-860. [doi:10.1080/02786826.2010.498455](https://doi.org/10.1080/02786826.2010.498455)
- [9] Risken, H. (1977) The Fokker-Planck equation. Springer-Verlag, Berlin.
- [10] Åkerstedt, H.O., Högberg, S.M. and Lundström, T.S. (2011) An asymptotic approach of Brownian deposition of nanofibers fibers in pipe flow. *Theoretical and Computational Fluid Dynamics*. <http://www.springerlink.com/content/101184/>
- [11] Åkerstedt, H.O., Högberg, S.M., Lundström, T.S. and Sandström, T. (2010) The effect of Cartilaginous rings on particle deposition by convection and Brownian diffusion. *Natural Science*, **2**, 769-779. [doi:10.4236/ns.2010.27097](https://doi.org/10.4236/ns.2010.27097)
- [12] Martonen, T.B., Yang, Y. and Xue, Z.Q. (1994) Influence of cartilaginous rings on tracheobronchial fluid dynamics. *Inhalation Toxicology*, **6**, 185-203. [doi:10.3109/08958379408995231](https://doi.org/10.3109/08958379408995231)
- [13] Zhang Y. and Finlay W.H. (2005) Measurement of the effect of cartilaginous rings on particle deposition in a proximal lung bifurcation model. *Aerosol Science and Technology*, **39**, 394-399. [doi:10.1080/027868290945785](https://doi.org/10.1080/027868290945785)
- [14] Etienne, S., Pierre, M. and Christian, D. (2010) Real time, nanometric 3D-tracking of nanoparticles made possible by second harmonic generation digital holographic microscopy. *Optics Express*, **18**, 17392-17403. [doi:10.1364/OE.18.017392](https://doi.org/10.1364/OE.18.017392)